Supplementary Information

Photocatalytic decarboxylative deuteration of lauric acid with heavy water for sustainable synthesis of deuterated alkanes

Haifan Huang,[a] Zihan Lin,[a] Akira Yamamoto,[a] Bhoi Yagna Prakash,[a] Kexin Zou,[a]
Shohichi Furukawa,[a] Ken-ichi Fujita,[a] Gunik Lee,[b] Jun Kumagai[c] and Hisao Yoshida*[a]

[a] Graduate School of Human and Environmental Studies, Kyoto University, Yoshida-nihonmatsu-cho, Sakyo-ku, Kyoto 606-8501, Japan

[b] Department of Material Chemistry, Graduate School of Engineering, Nagoya University, Chikusa, Nagoya 464-8603, Japan

[c] Institute of Materials and Systems for Sustainability Division of Materials Research, Nagoya University, Furo-cho, Chikusa-ku, Nagoya, Aichi 464-8601, Japan

* Corresponding author: yoshida.hisao.2a@kyoto-u.ac.jp

Contents

1. Methods

1.1 Synthesis deuterated *n*-undecane by Grignard reagent

Deuterated *n*-undecane (*n*-undecane-*d*) was synthesized as a reference compound using Grignard reagent (Scheme S1).[S1] A 50 ml solution of 1-chloroundecane ($CH_3(CH_2)_{10}Cl$) in diethyl ether (2.5 mol/L) was introduced into an argon-purged Schlenk tube. Separately, 18.75 mmol of magnesium (Mg) powder and 5–7 iodine (I_2) beads were placed in an eggplant flask and purged with argon. The flask was gently heated with the dryer to activate the iodine through evaporation. To initiate the reaction, 5 mL of the prepared 1-chloroundecane ether solution was carefully added dropwise via syringe while monitoring the reaction temperature to prevent runaway conditions. The remaining 45 mL of the solution was then added smoothly. The reaction mixture was stirred at room temperature for 1.5 h to generate the Grignard reagent ($CH_3(CH_2)_{10}ClMg$). Subsequently, 2 ml heavy water (D_2O) was injected to quench the Grignard reagent, yielding *n*-undecane-d_1. To ensure safety and manage the exothermic nature of the reaction, the flask was cooled with an ice water bath. After the completion of cooling, the mixture was filtered, dehydrated with sodium sulfate (Na_2SO_4), and filtered again. The ether solvent was then evaporated to isolate the synthesized *n*-undecane-d_1 as the final product.

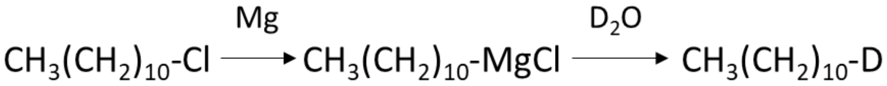

$$CH_3(CH_2)_{10}\text{-}Cl \xrightarrow{Mg} CH_3(CH_2)_{10}\text{-}MgCl \xrightarrow{D_2O} CH_3(CH_2)_{10}\text{-}D$$

Scheme S1 Synthesis of deuterated *n*-undecane by using Grignard reagent.[S1]

The product was confirmed by ^{13}C and ^{1}H NMR and MS(EI). The data of the product is as follows:

Deuterated undecane (*n*-undecane-1-*d*, $C_{11}H_{23}D$) synthesized using Grignard reagent: ^{1}H NMR (500 MHz, $CDCl_3$) δ 1.26 (m, 18H), 0.88 (t, J = 7.0 Hz, 5H). ^{13}C NMR (100 MHz, $CDCl_3$) δ 31.93, 31.90, 29.72, 29.67 (2C), 29.38 (2C), 22.70, 22.62, 14.14, 13.85 (t, J = 28.6, C-D). MS (EI): m/z: 157.[S2]

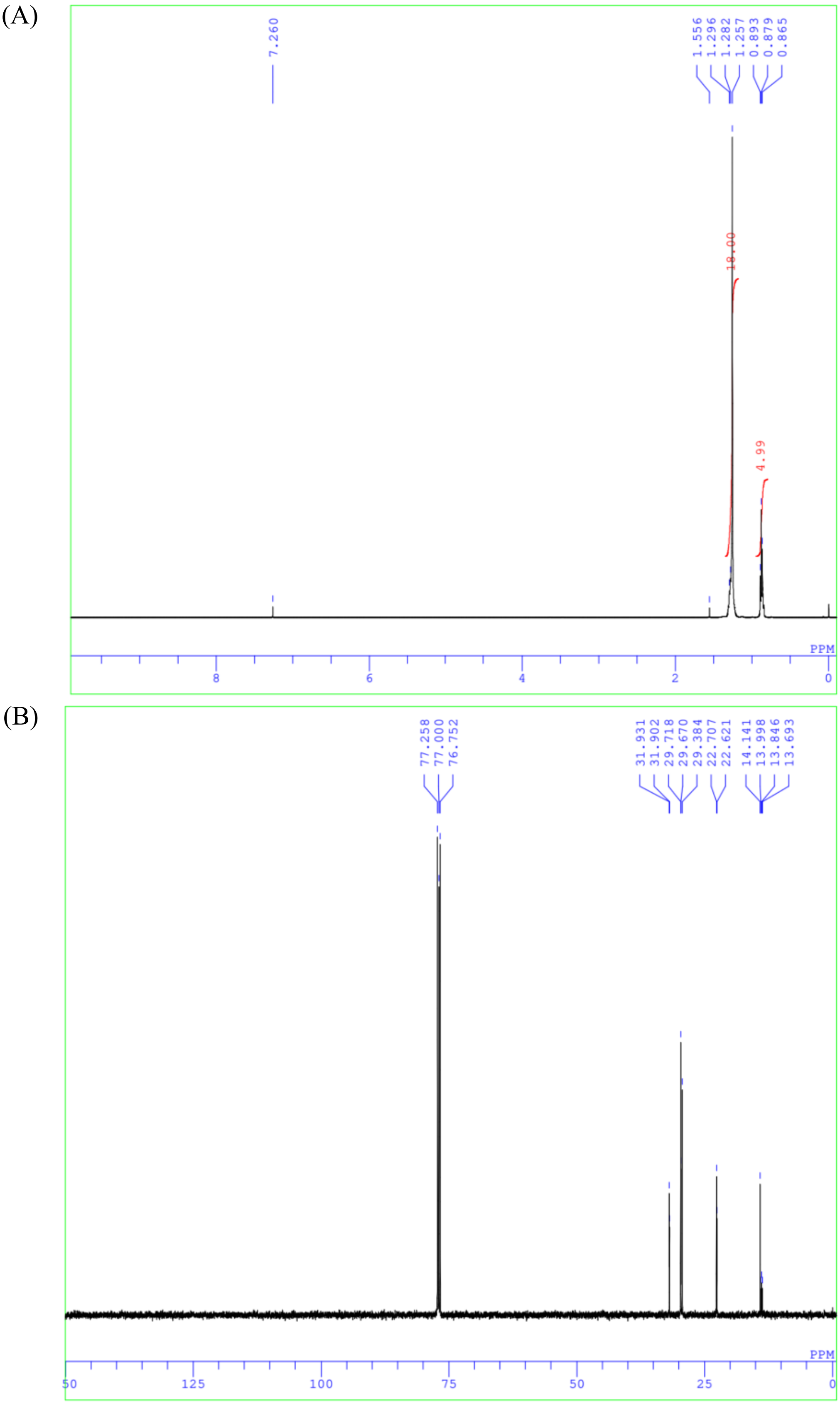

Fig. S1 NMR spectra of the deuterated undecane ($C_{11}H_{23}D$) synthesized using Grignard reagent: (A) ^{1}H NMR (500 MHz, $CDCl_3$) and (B) ^{13}C NMR (100 MHz, $CDCl_3$).

1.2 Analysis of deuterated compounds and isomers

GC-FID and GC-MS were used to determine the amount of deuterated undecane. Fig. S2a and Fig. S2b show the chromatograms of GC-FID and GC-MS, respectively, recorded for the products in a photocatalytic reaction test (3 h, 50mg of Au(0.1)/TiO_2, λ >360 nm). The peaks for the reactants and products appeared in the same order in both chromatograms.

In the total ion chromatogram of GC-MS (Fig. S2b, black line), a peak was observed at a retention time of 8.0 min, which was assigned to *n*-undecane ($C_{11}H_{24}$, m/z=156). Corresponding peak was also detected in each chromatogram of m/z=155, 156, and 157. These peaks were close to the mass number of *n*-undecane, although they displayed slightly different retention times (ranging from 8.2 to 8.25 min). This observation suggests that at least two compounds contributed to these peaks, as shown in Fig. S2c.

The commercially obtained *n*-undecane-d_0 (mass number=156) produced peaks at the retention time corresponding to m/z=156 (major) and 157. No peak was observed in the chromatogram for m/z=155 (Fig. S2d) while the *n*-undecane-d_1 (mass number=157) synthesized using the Grignard reagent (Scheme S1) exhibited one peak in each chromatogram for m/z=157 (major), m/z=158 (minor), and m/z=156 (very minor) as shown in Fig. S2e. The small peak at m/z=156 appeared at a slightly different retention time, assignable to *n*-undecane-d_0 as a byproduct formed during synthesis. It is noted that while both *n*-undecane-d_0 and *n*-undecane-d_1 displayed the main peaks in their respective chromatograms for m/z=156 and m/z=157, they also exhibited minor peaks at m/z=157 and m/z=158, respectively. Consequently, the peak at m/z=157 is unsuitable for quantitative analysis. Furthermore, the peak at m/z=158 consisted of multiple overlapping peaks and did not consistently yield a linear calibration curve. This suggests the presence of multiple compounds, such as *n*-undecane-d_2. Given these limitations, the peak area of m/z=156 was used to quantify the concentration of *n*-undecane-d_0 ($A_{\mathrm{C11\text{-}h}}$). The concentration of *n*-undecane-*d* ($A_{\mathrm{C11\text{-}d}}$) was determined by subtracting $A_{\mathrm{C11\text{-}h}}$ from the total concentration of *n*-undecane (A_{sum}, the sum of $A_{\mathrm{C11\text{-}h}}$ and $A_{\mathrm{C11\text{-}d}}$), as measured by GC-FID (Fig. S2a, C_{11}). This calculation is expressed in Eq. S1.

$$A_{\mathrm{C11\text{-}d}} = A_{\mathrm{sum}}\ \text{(from GC-FID)} - A_{\mathrm{C11\text{-}h}}\ \text{(from GC-MS)} \qquad \text{(S1)}$$

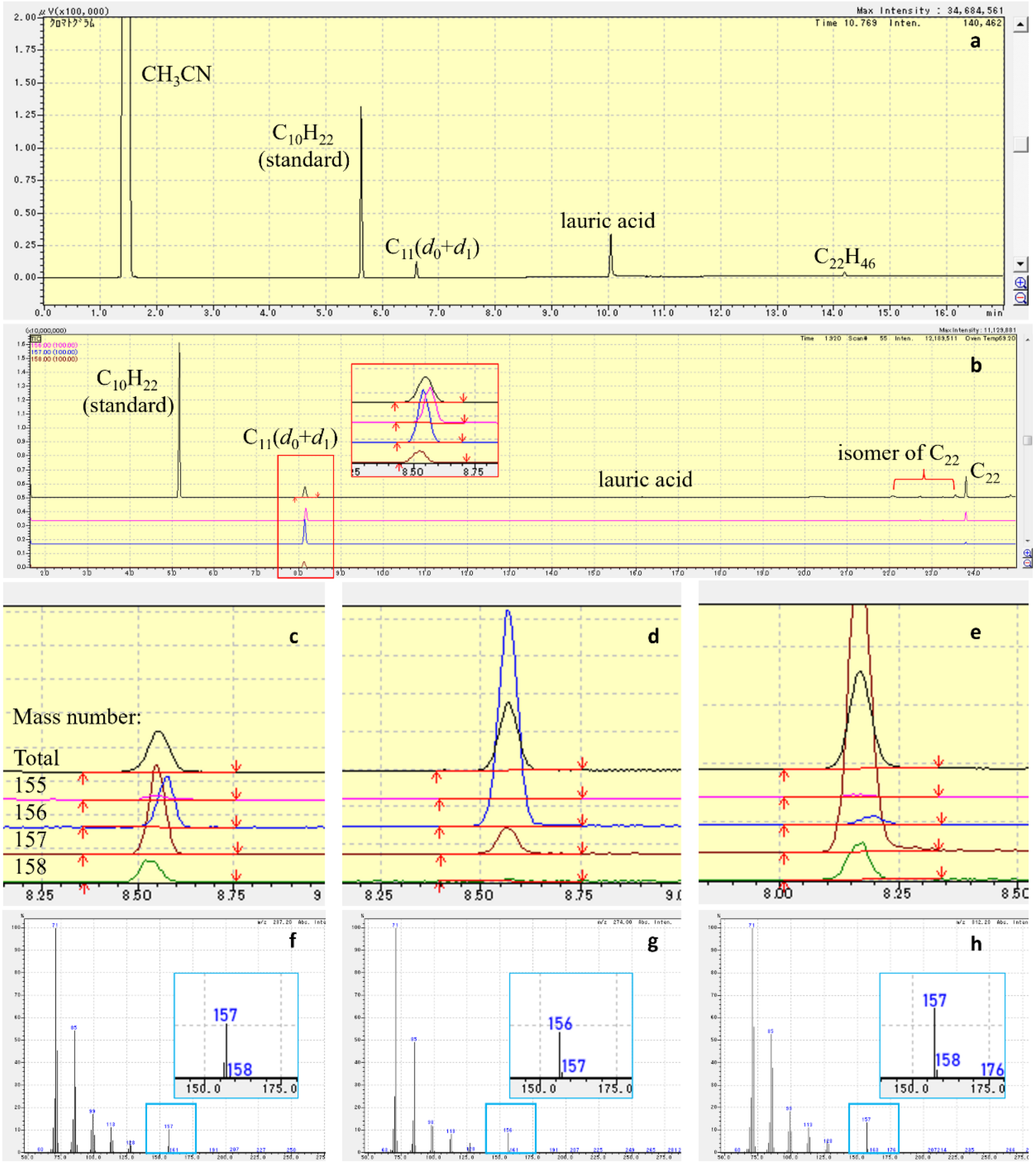

Fig. S2 Chromatogram of GC-FID (a), and total ion chromatogram of GC-MS of the obtained product solution (b), and the ion chromatograms for some m/z (total, and 155-158) at the peak for *n*-undecane in the product solution (c), commercially obtained *n*-undecane-*h* (d), and synthesized *n*- undecane-*d* (e), where the intensity of the chromatograms for each m/e was enlarged 100 times. MS spectra of the peak for *n*-undecane in the product solution (f), the commercially obtained *n*-undecane-*h* (g), and synthesized *n*- undecane-*d* (h) were also shown.

$$2\ C_9H_{19}CH_2{}^{\bullet}CH_2 \longrightarrow C_9H_{19}CH_2CH_2CH_2CH_2C_9H_{19} \tag{a}$$

$$C_9H_{19}CH_2{}^{\bullet}CH_2 + C_9H_{19}{}^{\bullet}CHCH_3 \longrightarrow C_9H_{19}CH(CH_3)CH_2CH_2C_9H_{19} \tag{b}$$

$$2C_9H_{19}{}^{\bullet}CHCH_3 \longrightarrow C_9H_{19}CH(CH_3)CH(CH_3)C_9H_{19} \tag{c}$$

$$C_9H_{19}CH(CH_3)CH(CH_3)C_9H_{19} \longrightarrow C_{22}H_{24} + H_2 \tag{d}$$

Scheme S2 Formation of C_{22} isomers, (a) coupling of two primary undecyl radicals, (b) coupling of primary and secondary undecyl radicals, (c) coupling of two secondary undecyl radicals, and (d) dehydrogenation of docosane to docosene.

In the total ion chromatogram of GC-MS (Fig. S2b), four peaks observed were assignable for isomers of C_{22} as byproducts, which would be produced from the coupling of two radical intermediates, i.e., primary and secondary undecyl radicals, ${}^{\bullet}C_{11}H_{23}$. This fact supports that the rearrangement of carbon radicals took place as well. Since the primary carbon radical is not as stable as the secondary one, radical rearrangement (intramolecular hydrogen atom transfer) can take place to form secondary radicals (See the main text). The coupling of two primary radicals gives *n*-docosane without blanch ($C_{22}H_{46}$, Scheme S2a), coupling of the primary and secondary radicals gives an isomer, 10-methylhenicosane ($C_9H_{19}CH(CH_3)C_{11}H_{23}$, Scheme S2b), and coupling of two secondary radicals leads to another isomer, 10,11-dimethylicosane ($C_9H_{19}CH(CH_3)CH(CH_3)C_9H_{19}$, Scheme S2c).

According to the retention time, the highest peak among the four peaks in the range for C_{20}–C_{22} hydrocarbons was assignable to *n*-docosane ($C_{22}H_{46}$, Scheme S2c). Other three peaks were detected with earlier retention times than the peak of *n*-docosane in GC-MS (Fig. S1b). Very small peaks with shorter retention times were assigned to the blanched isomers with shorter main carbon chains (Scheme S2b and c), suggesting these were formed from the secondary radical(s). MS indicated the presence of an alkene ($C_{22}H_{44}$), suggesting a possible dehydrogenation route for alkene formation from C_{22} as shown in scheme S2d. In conclusion, isomers of docosane and further dehydrogenated product were confirmed, which should be formed by coupling of the undecyl radicals.

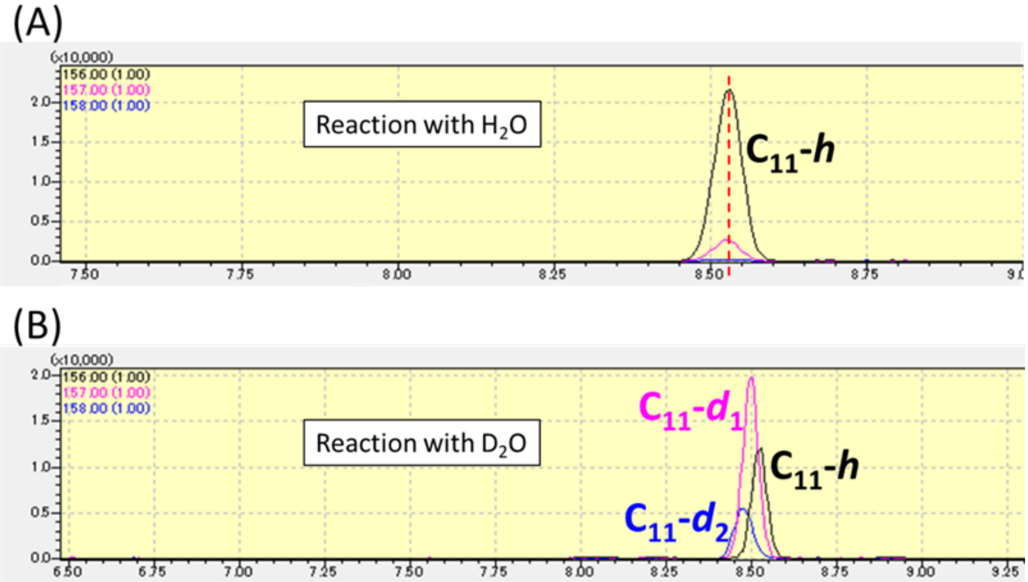

Fig. S3 The GC-MS total ion chromatograms of the obtained product solution from the photocatalytic reaction test of LA decarboxylation using (A) H_2O and (B) D_2O.

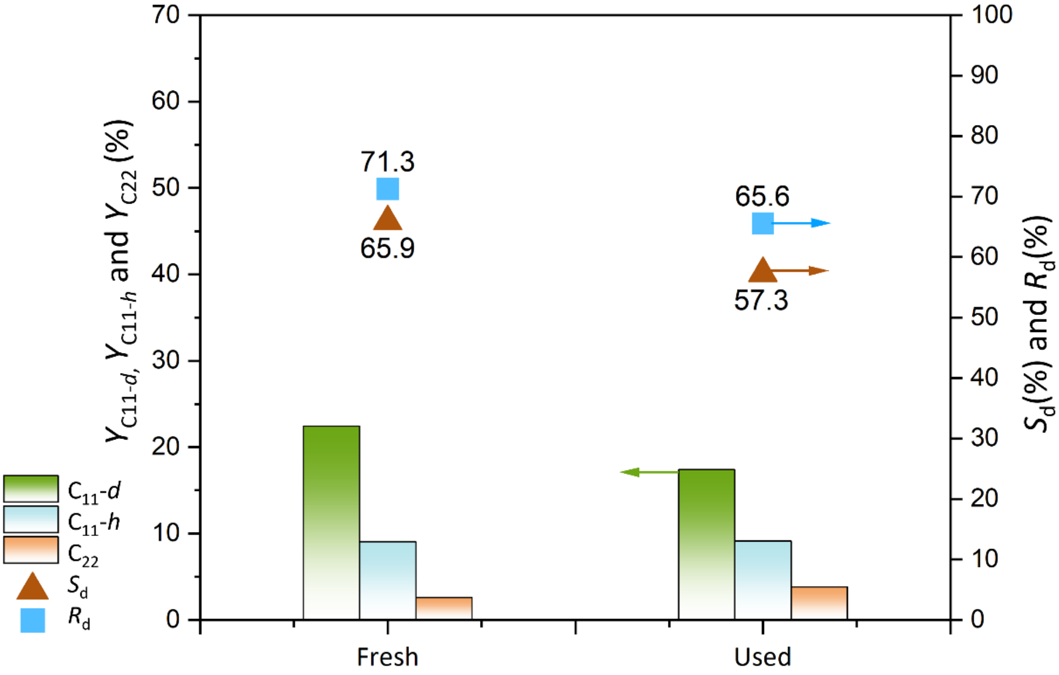

Fig. S4 Reuse test of photocatalytic lauric acid conversion over the Au(0.5)/TiO_2 sample. Find the experiment conditions for the first run in Table S7, entry d. After the first run, the photocatalyst was washed with CH_3CN, followed by the second run without any pretreatment.

A reuse test was conducted. The same catalyst was used in two successive reaction runs. After the first reaction, the catalyst was washed three times with acetonitrile. For the second run, pre-heating and pre-irradiation were not conducted. As a result, the deuterated alkane was successively obtained (Fig. S4). However, the yield of the target product, C_{11}-d, was found to have slightly decreased in the second run with the reused catalyst. R_d value was reduced from 71.3% to 65.6%. Notably, the used catalyst showed a lighter color than its initial purple tone. During the reaction process, the co-catalyst structure may have undergone changes or that the light-absorbing components may have been lost. Possible causes include aggregation of Au metal nanoparticles, localized leaching of active components, or contamination and blocking of active sites by organic byproducts on the surface. To improve the durability of the catalysts, further effort should be paid on the following aspects: the process of the catalyst recycling, catalyst surface modification, and the improving property of the loaded co-catalyst metals.

2. Supplementary Results in Tables

Table S1 Photocatalytic decarboxylation deuteration of lauric acid over various catalyst samples [a].

		Product [c] (μmol)						
Entry	Catalyst [b]	C_{11}-*d*	C_{11}-*h*	C_{22}	$Y_{C11\text{-}d}$ (%) [d]	Y_{total}(%) [e]	S_d (%) [f]	R_d (%) [g]
1	TiO_2	1.10	0.587	0.271	2.20	4.46	49.3	65.2
2	Au(0.1)/TiO_2	1.75	0.598	0.451	3.50	6.50	53.8	74.5
3	Pt(0.1)/TiO_2	2.42	1.05	1.48	4.84	12.86	37.6	69.7
4	Pd(0.1)/TiO_2	3.34	1.54	0.691	6.68	12.52	53.3	68.4

[a] Reaction conditions; catalyst 50 mg, the reaction mixture (5 mL) containing LA 40 mg (50 μmol), in D_2O (3 mL) and CH_3CN (2 mL), reaction time 0.5 h, light wavelength > 360 nm, irradiated light intensity 41 mW·cm^{-2} when measured at 360 ± 20 nm. [b] ST-01 anatase. [c] C_{11}-d_1 = n-undecane-d_1, $C_{11}H_{23}D$, C_{11}-d_0 = n-undecane-d_0, $C_{11}H_{24}$, C_{22} = n-docosane; [d] Yield of *n*-undecane-d_1, $Y_{C11\text{-}d1}$ (%) = 100 × $A_{\text{undecane-d1}}$/ $A_{\text{initial lauric acid}}$; [e] Y_{total} (%) = 100 × ($A_{\text{undecane-d1}}$+ $A_{\text{undecane-d0}}$ + 2×A_{docosane})/$A_{\text{initial lauric acid}}$ [f] Selectivity of $C_{11\text{-}d1}$ to the obtained main products (C_{11} and C_{22}) S_d (%)=100 × $A_{\text{undecane-d1}}$ /($A_{\text{undecane-d0}}$ + $A_{\text{undecane-d1}}$ + 2×A_{docosane}). [g] Ratio of undecane-d_1 to sum of undecane-d_1 and undecane-d_0, R_d(%)=100 × $A_{\text{undecane-d1}}$/($A_{\text{undecane-d0}}$+ $A_{\text{undecane-d1}}$).

Table S2 Results of the blank tests. [a]

			Product yield (%) [b]		
Entry	Photoirradiation	Photocatalyst	C_{11}-*d*	C_{11}-*h*	C_{22}
1	No	No	n.d. [c]	n.d.	n.d.
2 [d]	No	Yes	n.d.	n.d.	n.d.
3 [e]	Yes	No	n.d.	n.d.	n.d.

[a] The reaction conditions and time are the same as in Table S1. [b] See the caption for Table S1. [c] n.d. = not detected. [d] Amount of the Au(0.1)/TiO_2 sample was 50 mg. [e] Incident light wavelength was > 360 nm; irradiated light intensity was 41 mW cm^{-2} when measured at 360 ± 20 nm.

Table S3 Results of the photocatalytic reaction test with various reaction times. [a]

		Product yield [b] (%)					
Entry	Time/hour	C_{11}-*d*	C_{11}-*h*	C_{22}	Y_{total} (%)	S_d (%)	R_d (%)
1	0.5	3.50	1.19	1.80	6.50	53.9	74.6
2	1	6.86	1.06	2.93	10.9	63.2	86.6
3	3	9.28	4.40	5.52	19.2	48.3	67.8
4	5	11.4	5.52	8.60	25.5	44.6	67.3
5	6	11.5	6.20	11.5	29.2	39.4	64.9

[a] Reaction conditions were the same as shown in Table S1, photocatalyst was 50 mg of the Au(0.1)/TiO_2 sample; [b] See the caption for Table S1; $Y_{C11\text{-}d}$ (%) = 100 × $A_{\text{undecane-d0}}$/ $A_{\text{initial lauric acid}}$; Y_{C22} (%) = 100 × 2× A_{docosane}/ $A_{\text{initial lauric acid}}$

Table S4 Photocatalytic deuteration of lauric acid over the Au(x)/TiO_2 samples [a]

Entry	Catalyst	Product yield (%)			Y_{total} (%)	S_{d} (%)	R_{d} (%)
		C_{11}-*d*	C_{11}-*h*	C_{22}			
1	Au(0.1)/TiO_2	9.26	4.40	5.52	19.2	48.3	67.8
2	Au(0.5)/TiO_2	15.7	3.92	8.96	28.6	54.9	80.0
3	Au(1.0)/TiO_2	6.68	3.08	5.96	15.7	42.5	68.5

[a] Reaction condition: the amount of catalyst was 50 mg, lauric acid (40 mg, 50 μmol) was used in a solution consisting of D_2O (3 mL), and acetonitrile (CH_3CN, 2 mL); reaction time was 3 h; incident light wavelength > 360 nm; irradiated light intensity was 41 mW·cm^{-2} when measured at 360±20 nm. See other caption in Table S1 and Table S3.

Table S5 Photocatalytic deuteration of lauric acid with different ratios of acetonitrile and D_2O [a]

Entry	D_2O:CH_3CN	Product yield (%)			Y_{total} (%)	S_{d} (%) [c]	R_{d} (%) [d]
		C_{11}-*d*	C_{11}-*h*	C_{22}			
1	2:3	4.09	6.08	1.89	12.1	33.9	40.2
2	1:1	8.92	6.16	3.50	18.6	48.0	59.2
3	3:2	16.4	3.10	3.41	22.9	71.6	84.1

[a] Reaction condition: the amount of catalyst was 50 mg, lauric acid (40 mg, 50 μmol) was used in a solution consisting of acetonitrile and D_2O with various ratios; reaction time was 3 h; the incident light wavelength was longer than 360 nm; irradiated light intensity was 41 mW·cm^{-2} when measured at 360±20 nm. Before the reaction, the catalysts were heated in an argon flow at 450 K for 0.5 h. Other reaction conditions are the same as mentioned in Table S4.

Table S6 Photocatalytic deuteration of lauric acid with various light irradiation intensities [a]

Entry	Light intensity (mW cm^{-2})	Product yield (%)			Y_{total} (%)	S_{d} (%)	R_{d} (%)
		C_{11}-*d*	C_{11}-*h*	C_{22}			
a	4.9	4.16	3.05	2.13	9.34	44.5	57.7
b	11.8	7.57	4.38	2.01	14.0	54.2	63.4
c	20.5	11.2	6.17	2.47	19.9	56.5	64.5
d	41.0	16.4	3.10	3.41	22.9	71.6	84.1

[a] Reaction conditions: the 50 mg of catalyst Au(0.5)/TiO_2 was used with different irradiation intensities from 4.9 mW·cm^{-2} to 41 mW·cm^{-2}. Before the reaction, the catalysts were heated in an argon flow at 450 K for 0.5 h. Other reaction conditions are the same as mentioned in Table S4.

Table S7 Photocatalytic deuteration of lauric acid over different pretreatment conditions [a]

Entry	Pretreatment		Product yield (%)			Y_{total} (%)	S_{d}(%)	R_{d}(%)
	heating	irradiation	C_{11}-*d*	C_{11}-*h*	C_{22}			
a	no	no	7.09	4.13	4.44	15.7	45.3	63.2
b	no	with D_2O	8.85	5.25	1.61	15.7	56.3	62.8
c	done	with D_2O	15.3	2.68	4.33	22.3	68.5	85.1
d	done	without D_2O	16.4	3.10	3.41	22.9	71.6	84.1

[a] Reaction conditions: the 50 mg of catalyst Au(0.5)/TiO_2 was used with the following conditions: (a,b) without or (c,d) with preheating; pre-irradiation in the (c) presence or (d) absence of D_2O. Other reaction conditions are the same as mentioned in Table S4.

Table S8 Photocatalytic deuteration of lauric acid over different solvents [a]

		Product yield (%)					
Entry	Component	C_{11}-*d*	C_{11}-*h*	C_{22}	Y_{total} (%)	S_d(%)	R_d(%)
a	D_2O/CH_3CN	16.4	3.10	3.41	22.9	71.6	84.1
b	D_2O/CD_3CN	19.4	5.05	3.84	28.3	68.6	79.3
c	H_2O/CD_3CN	0	26.2	2.94	29.2	0	0
d	H_2O/CH_3CN	0	27.5	2.84	30.3	0	0

[a] The catalyst was 50 mg of Au(0.5)/TiO_2, lauric acid (40 mg, 50 μmol) was used in a solution consisting of CH_3CN/CD_3CN (2 mL) and H_2O/D_2O (3 mL). Other conditions are the same as in Table S7, entry d.

Table S9 Relative enthalpy [a] of undecyl radical ($^{\bullet}C_{11}H_{23}$) having a radical center at the *n*-th carbon from the terminal one in linear undecyl radical, $CH_3(CH_2)_x{}^{\bullet}CH(CH_2)_{8-x}CH_3$ (x=0–3, corresponding to n=2–5), calculated by Gaussian 16. [S3]

n	1st	2nd	3rd	4th	5th
ΔH / kJ·mol^{-1}	0	−6.95	−5.40	−5.24	−5.08

[a] Optimized structure of corresponding linear undecyl radicals in water and their vibrational frequencies without negative ones were calculated by ump2(full)/aug-cc-pvdz method by Gaussian 16.[S3] All linear undecyl radicals are assumed to be in *trans* structures.

References

S1 A. A. Leushukou, A. V. Krech and A. L. Hurski, *Org. Lett.*, 2022, **24**, 6277–6281.

S2 Y. L. Sun, F. F. Tan, R. G. Hu, et al., *Chin. J. Chem.*, 2022, **40**, 1903–1908.

S3 M. J. Frisch, G. W. Trucks, H. B. Schlegel, G. E. Scuseria, M. A. Robb, J. R. Cheeseman, G. Scalmani, V. Barone, G. A. Petersson, H. Nakatsuji, et al. Gaussian 16, Revision C.02; Gaussian, Inc.: Wallingford CT, 2019.